

Dear Dr. Tian,

We would like to thank you and the two reviewers for your reviews of our manuscript “Emergent stationarity in Yellow River sediment transport and the underlying shift of dominance: from streamflow to vegetation”. We appreciate these insightful inputs that have helped to improve the quality of this manuscript. In response to the comments, we have made corresponding revisions. Our response to each comment is listed below in blue with the specific line numbers of the changes we have made. Again, we appreciate the time and inputs from you and the reviewers.

Best regards,
Sheng Ye,
Qihua Ran,
Xudong Fu,
Chunhong Hu,
Guangqian Wang,
Gary Parker,
Xiuxiu Chen,
Siwei Zhang

Anonymous Referee #1

Received and published: 16 August 2018

The authors collected and analyzed hydrologic data to develop the relationships between sediment concentration and discharge, vegetation index and discharge and sediment concentration in the Yellow River Basin using Wavelet Coherence method. Eventually they drew some conclusions on these relationships. Both data and analysis well support these conclusions. The reviewer recommends to accept the paper with some minor revisions as follows,

We appreciate the reviewer’s insightful inputs that have helped to improve the quality of this manuscript. In response to the comments, we have made corresponding revisions. Our response to each comment is listed below in blue with the changes in manuscript, we also include the specific line numbers of the changes we have made. We hope the reviewer find the revision and responses sufficient.

1. Double check the whole manuscript and correct some typos such as: Line 108 (“”) is expected in Eqn 1), Line 121, “the” strongest. . . etc.

We have corrected the typos as following, thank you (please see lines 116 and 135).

$$L116: R^2(s) = \frac{|S(s^{-1}W^{XY}(s))|^2}{S(s^{-1}|W^X(s)|^2) \cdot S(s^{-1}|W^Y(s)|^2)}$$

L135: “This analysis is applied only at annual scale since this is when the coupling from wavelet coherence analysis is the strongest.”

2. Lines 118 – 129, use formula instead of description to explain the physical meaning of these parameters.

We have now replaced the description of the parameters by equations as following, thank you (please see lines 126 – 144).

The annual discharge (Q_a) and the sediment yield (L_a) were aggregated from daily to further examine their correlation:

$$Q_a = (\sum_{i=1}^n (Q_i * 3600 * 24)) / Ad * 1000 \quad (2)$$

$$L_a = (\sum_{i=1}^n (Q_i * C_i * 3600 * 24)) \quad (3)$$

where Q_i (m^3/s) and C_i (kg/m^3) are the daily discharge and sediment concentration, Ad is the drainage area (km^2) of each gauge, n is the number of days in each year. This analysis is applied only at annual scale since this is when the coupling from wavelet coherence analysis is the strongest. The annual mean concentration (C_a) was calculated as:

$$C_a = L_a / (Q_a * Ad / 1000) \quad (4)$$

The long-term mean annual discharge (Q_m) and the long-term mean annual concentration (C_m) was also calculated by averaging for the period of 1951 to 1986. Note that both the parameters Q_a and Q_m used here are area-specific discharges (mm/yr). For each gauge, a linear regression was fit to describe the correlation between annual discharge (Q_a) and annual mean concentration (C_a). The slope of this linear regression (α_{QC}) is used to describe the rate of change in sediment concentration with changing discharge at annual scale.

3. Even though NVDI has been described in the cited literature, it will be more convenient for readers understand the effect of vegetation if the authors can briefly explain the definition.

We have added following brief explanation on NDVI in the manuscript, we hope the reviewer find this satisfactory (please see lines 90 – 95).

The vegetation data used in this study corresponds to the normalized difference vegetation index (NDVI), which is an index calculated from remote sensing measurements to indicate the density of plant growth (Running et al., 2004). The NDVI data was downloaded from NASA's Land Long Term Data Record (LTDR) project, which provides daily NDVI observations globally at a spatial resolution of 0.05° .

4. More discussion on the determination of threshold value of discharge is expected.

We obtained the threshold value of discharge by the slope in the Q-C regression (α_{QC}), $60mm/yr$ is where most α_{QC} is less than 0.1 while $100mm/yr$ is where most α_{QC} is less than 0.01. Those gauges with larger mean annual discharge are the ones downstream of the major tributaries or along the main stem of YR. For these gauges, due to the larger drainage area, there is significant heterogeneity in the catchments. The region generates more discharge doesn't necessary contribute most in sediment yield (Figure S4), factors other than discharge may play important roles. This

threshold discharge was also found in arid watersheds in Arizona though with quite different numbers. This divergence could be attributed to the different catchment characteristics like soil type, topography and so on. It would be interesting to further study the cause of the threshold discharge at these specific values, but this is above the scope of this work and we will pursue this in our follow-up studies. We have now added the following discussion in the manuscript. Hopefully the reviewer finds it sufficient (please see lines 166 – 172 and 346 - 348).

L166: For example, gauges with α_{QC} less than 0.1 are the ones with Q_m larger than 60mm/yr. When Q_m is larger than 100mm/yr, the variation in sediment concentration is less than 1% of that in streamflow ($\alpha_{QC} < 0.01$), and thus sediment concentration can be approximated as invariant to changing discharge. Most of these gauges locate on the main stem or near the outlets of tributaries. This increased independence between sediment concentration and discharge may be attributed to the heterogeneity in these relatively large catchments.

L346: Analysis with more field measurements could also help explain the threshold discharge of the emergent stationarity.

5. How will vegetation type, climate, and other watershed characteristics affect the conclusion? A short discussion will be helpful.

The vegetation types in the YRB include bare soil, grassland, shrubs and forest (Zhang et al., 2016), our conclusion is derived from these various vegetation types. But we only look at the NDVI in this study, it is possible that the capability to prevent soil erosion may vary with vegetation species despite of similar NDVI values. This worth exploring with more detailed studies in the future. On the other hand, the climate in the YRB is semi-arid and arid (mean annual precipitation varies within the range of 100mm to 800mm), it would be interesting to see whether our conclusion would sustain under humid climate. Although catchments with humid climate usually have well-developed vegetation coverage, thus the soil erosion issue is less severe, there could still be soil erosion problems. Thus, it would be interesting to study the soil erosion issue in those humid catchments. We have included the following discussion on this in the manuscript, we hope the reviewer will be satisfied with it (please see lines 342 – 346).

It will be helpful if we could examine our findings in other watersheds worldwide with different climate and vegetation types. Although humid regions are usually considered as well-vegetated, study shows that there could still be erosion issues in these areas due to topographic gradient, precipitation intensity, and soil properties, etc. (Holz et al., 2015).

Anonymous Referee #2

Received and published: 29 October 2018

General comments: The authors quantified the annual impacts of discharge and vegetation density on the sediment concentration at dozens of gauges over the Yellow River basin. The conclusion is that the dominant controlling factor of sediment shifts from discharge to the vegetation resistance with discharge increasing, which is interesting. Besides, the manuscript was well written. However, some problems about the details of the assumptions and method used (i.e. wavelet coherence analysis and regression fitness) are expected to be explained more clearly, as these details are very critical to the reliability as well as reasonableness of results associated with main conclusion.

We appreciate the reviewer's comments and have made our efforts to explain our assumptions and method used in the manuscript as the reviewer suggested. Our response to each comment is listed below in blue with the changes in manuscript, we also include the specific line numbers of the changes we have made. We hope the reviewer find the revision and responses satisfactory.

Several detailed comments are listed as follows:

(1) "The sediment concentration follows a bell shape with NDVI at annual scale" was summarized throughout the text (e.g., Line 12/193/253), while the log-transformation was used to sediment concentration data in Figures 2 and 3. As we know, the log transformation is non-linear, thus the bell shape in Figures 2 and 3 may depend on this transformation approach.

We agree with the reviewer that log-transformation would change the shape of the correlation between NDVI and concentration. But as we shown here the increase and decrease trend of the bell shape sustains and is clear in linear scale. As the concentration covers a large range from 0.1kg/m^3 to 700kg/m^3 , the points with small concentration (i.e. $\leq 100\text{kg/m}^3$) would all collapse. The differences among these points cannot be shown clearly in linear scale. Thus, to make the relationship clearer we choose the log-transformation for better presentation. We hope the reviewer finds our explanation satisfactory.

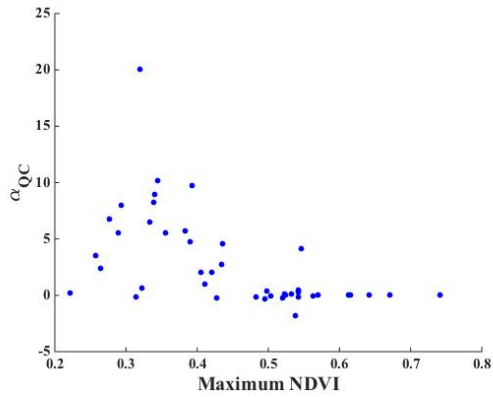


Figure 2R1: Scatter plots between the maximum NDVI and slope in the Q-C regression (α_{QC}).

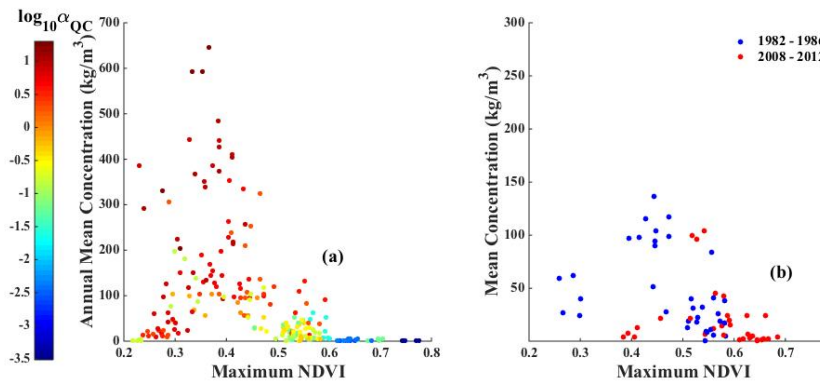


Figure 3R1: Scatter plot of annual mean concentration and maximum NDVI: (a) at 44 study gauges between 1982 and 1986, where the dots are color-coded by the slope in the Q-C regression (α_{QC}) at each gauge; and (b) at 7 gauges with both data from the years 1982 – 1986 (blue dots) and the years 2008 – 2012 (red dots).

(2) In Figure 3, the authors should give the mathematical expression of the fitted curve with bell shape. Is it of a polynomial form or something else? Moreover, the goodness of the fit is expected to be presented.

Yes, it is a polynomial form. We have now shown the mathematical expression of the fitted curve, as well as the goodness of the fit in the figure. Thank you for your suggestion (please see the updated Figure 3).

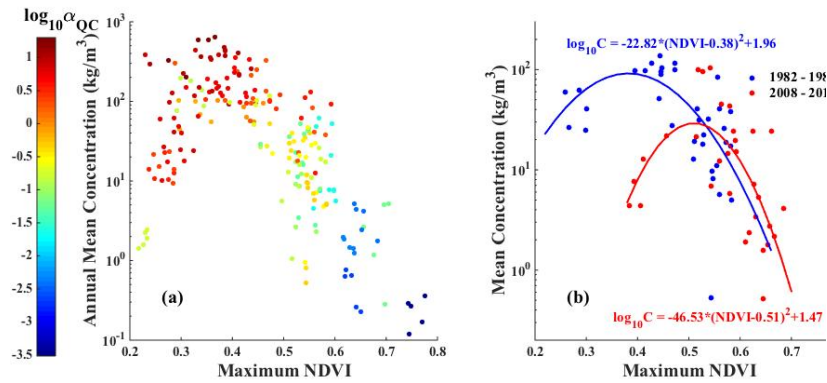


Figure 3R2: Scatter plot of annual mean concentration and maximum NDVI: (a) at 44 study gauges between 1982 and 1986, where the dots are color-coded by the slope in the Q-C regression (α_{QC}) at each gauge; and (b) at 7 gauges with both data from the years 1982 – 1986 (blue dots) and the years 2008 – 2012 (red dots). The R^2 for the two fit is 0.6 and 0.44 respectively with p -value < 0.001 for both of them.

(3) It's doubtful that the so-called emergent stationarity is attributed only to vegetation resistance. The physical connection between vegetation condition and sediment concentration is not as explicit as that between discharge and sediment concentration. In addition, the discharge and the vegetation were separately incorporated to consider the impact to sediment condition. So, the conclusion in this study is under very strong assumption, i.e., the sediment condition in a basin is only controlled by discharge and vegetation. However, this assumption was not listed clearly. On the other hand, was it reasonable? In addition to vegetation, resistance of sediment to erosion may be related to other property of the basin, such as soil properties. Authors said sediment concentration follows a bell shape with vegetation index. I guess that the mean sediment concentration also follows a bell shape with the mean runoff. According to literatures, the discharge of 1982-1986 in many sub-basins of Yellow River was much larger than that in 2008-2012, how to compare the decreased discharge contribution with the increased NDVI contribution to the concentration? Can the authors add the plot of mean sediment concentration against annual discharge with the same period and gauges in both Figure 3a and 3b?

We are sorry about the confusion we made that “the sediment condition in a basin is only controlled by discharge and vegetation.” What we are trying to say in this manuscript is that based on our findings of the correlation between NDVI and concentration from the data, vegetation plays an important role in soil erosion and sediment transport for all the study catchments. Combining with Figure 1 that the coupling between Q-C weakens with the increase in mean annual discharge, we have the results that: when mean annual discharge is small, both discharge and vegetation have good correlation with sediment concentration, while when mean annual discharge is relatively large, the correlation between vegetation and concentration sustains, but the correlation between Q-C fades out. For the former situation (mean annual discharge is small), Q-C is positively correlated, which is consistent with our intuitive that larger discharge delivered more

sediment. While the positive correlation between NDVI and concentration is counterintuitive, as we usually think vegetation helps prevent soil erosion. Thus, we think for these catchments, the increase in concentration is caused by hydraulic erosion and transport. Although larger Q also enables growth in vegetation, the amount of vegetation coverage is not sufficient to resist soil erosion caused by discharge. That is, the correlation between NDVI and concentration for these gauges is not a causal relationship, but is more likely because of the discharge. On the other hand, for the latter condition when mean annual discharge is relatively large, the impact of discharge disappears while the resistance from vegetation takes the dominance. But as the reviewer pointed out that our understanding in physical connection between vegetation condition and sediment concentration is not as explicit as that between Q - C . Further studies on the physical impact of vegetation is essential to explain this bell shape correlation in the perspective of mechanism. Indeed, motivated by this finding, we have done numerical simulations on the change in soil properties like saturated hydraulic conductivity caused by re-vegetation in another manuscript forthcoming.

We have also studied the correlation between dominant soil types and sediment concentration, the plot is quite scatter, thus we didn't show it in the manuscript for brevity. The results is shown in Figure R1. It is possible that there are other factors we did't consider here that influences the sediment transport, however, given the good fit between maximum NDVI and concentration, it is reasonable to say that vegetation plays an significant role in the soil erosion and sediment transport in the YRB, though it may not be the only controlling factor.

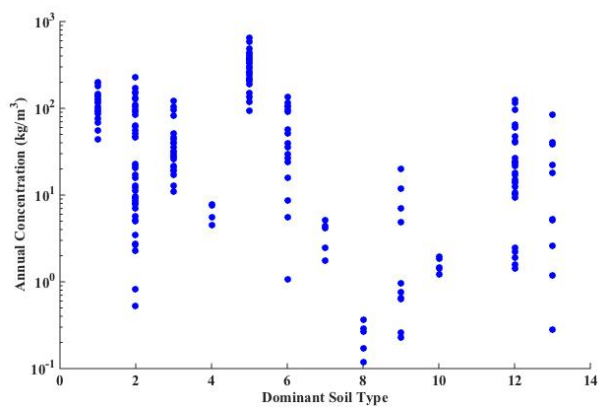


Figure R1: Scatter plot of annual mean concentration and dominant soil types: the denotations are as follows: 1: hilly gully region 1; 2: hilly gully region 2; 3: hilly gully region 3; 4: hilly gully region 4; 5: hilly gully region 5; 6: plateau gullies; 7: terrace; 8: alluvial plain; 9: stony mountains; 10: highland grassland; 11: dry grassland; 12: sandy; 13: hilly woods.

The relationship between annual discharge and concentration is shown in Figure 3R3. As we can see from Figure 3R3a, instead of a bell shape correlation, the mean concentration generally declines with annual discharge for all the 68 study gauges. However, this trend doesn't sustain for the seven gauges at the outlet of major tributaries (Figure 3R3b), where the plot is more scatter.

This is consistent with our findings in Figure 1b, that these gauges near the outlet of tributaries have less coupled discharge-concentration relationship. Although the discharge of 1982 – 1986 is smaller than that in 2008 – 2012, we believe the strength of the correlation between Q-C would sustain. Moreover, from Figure 1b, we can see that usually catchments with smaller discharge have stronger Q-C correlation. As we can from Figure 3R3b, the plots are scatter in both 1982 – 1986 and 2008 – 2012 despite of the change in discharge. Thus, we think that the vegetation is a better indicator of concentration than discharge.

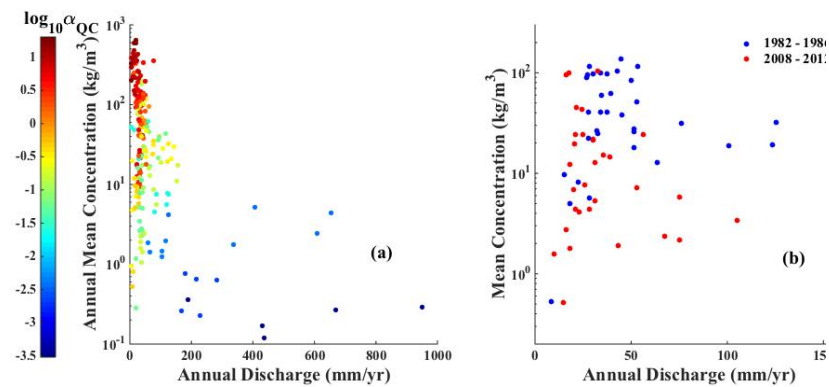


Figure 3R3: Scatter plot of annual mean concentration and annual discharge: (a) at 44 study gauges between 1982 and 1986, where the dots are color-coded by the slope in the Q-C regression (α_{QC}) at each gauge; and (b) at 7 gauges with both data from the years 1982 – 1986 (blue dots) and the years 2008 – 2012 (red dots).

We have added the following explanation in different parts of the manuscript (please see lines 229 – 235 and 348 – 352), we hope the reviewer finds our explanation satisfactory.

L229: To confirm this impact of vegetation resistance, we also examined the relationship between sediment concentration and other catchment characteristic like dominant soil type. No significant correlation was observed as vegetation did. Although there could still be other factors not considered here contributed to the decline in sediment concentration, it is undoubted that vegetation is one of the most influential factors of sediment reduction and can be used as a good indicator of the soil erosion and sediment transport in the YRB.

L348: Numerical simulations as well as long-term measurements on the soil properties are also needed to further explain the physical mechanism of vegetation retardation: how it develops its impact on soil erosion and sediment transport by changing soil properties and other topographic characteristics during its growth and spread.

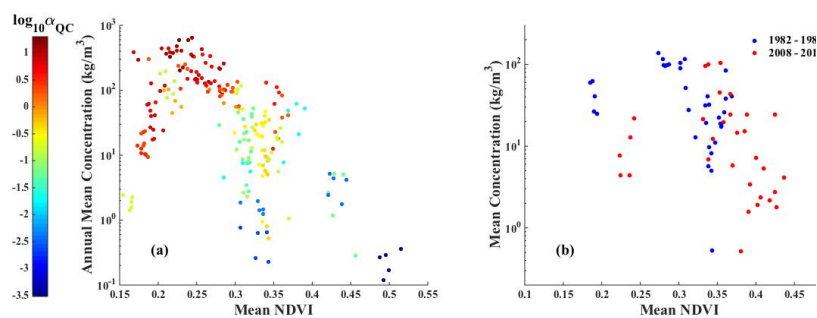
(4) On line 92-96 about the NDVI data used, how area-specific NDVI was obtained from the spatial imagery? Since the downloaded imagery was global, why only NDVI at 44 gauges not the maximum 68 gauges was estimated.

We extracted the raster data of NDVI from the global image by the drainage area of each gauge. Instead of the 68 gauges, we choose to use the 44 gauges located on the major tributaries for further study, as the water and sediment relationship at gauges on the main stem are more likely to be significantly influenced by the major dams along the YR. The situations on hillslope in the catchments could be overwhelmed by these dam activities. To avoid the significant impact from the human management on water release, we chose these 44 gauges on the major tributaries for our further analysis on the catchment characteristics. We hope the reviewer satisfies with our explanation (please see lines 99 – 101). The following is the explanation we added in the manuscript:

The gauges on the main stem of YR were not used as the water and sediment condition there is more likely controlled by the major dams along the main stem rather than the hillslope characteristics.

(5) Why not use the mean NDVI, but the maximum (daily?) NDVI, when you investigated the relationship between the NDVI and mean concentration at annual scale? How much uncertainty for the maximum NDVI exists?

We tried the mean NDVI as well, the rising and falling trend is still apparent (see following figure), but the maximum NDVI provides better shape. Thus, we chose to use the maximum NDVI for presentation. One possible reason is that the vegetation types in the YRB are mostly deciduous, the green period is relatively short, an averaged NDVI could decrease the difference among vegetation density. Since the variability in maximum NDVI for each site is not very large (Figure 3a), and the trend is consistent between mean NDVI and maximum NDVI, we think the uncertainty for the maximum NDVI is not significant for this study. We hope the reviewer finds our explanation sufficient.



(6) In Figure A1, the text in legend is inappropriate, because there were not 68 green triangles plotted (maybe 68-44=22 gauges).

Since the 44 gauges belongs to the 68 gauges, it might be confusing to use 22, we have changed the symbol to make it clear. Hopefully the reviewer finds the updated figure appropriate.

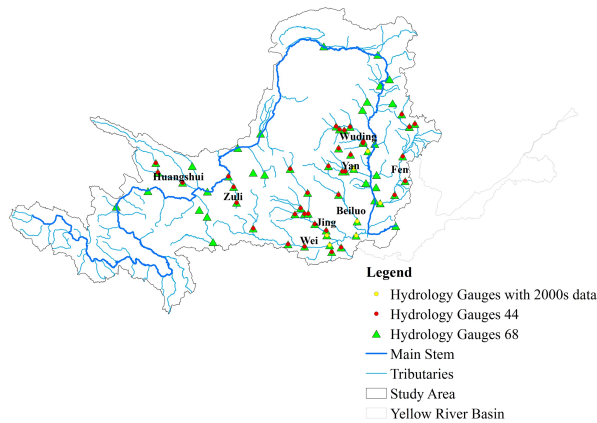


Figure S1: Spatial distribution of hydrology gauges used in this study. The green triangles correspond to 68 gauges with discharge and sediment concentration data, the red circles correspond to 44 selected gauges with NDVI data, and the yellow circles are the ones with annual discharge and sediment data for the years 2000 – 2012.

(7) On line 120, “annual scale . . . is when the coupling from wavelet coherence analysis is strongest”, why?

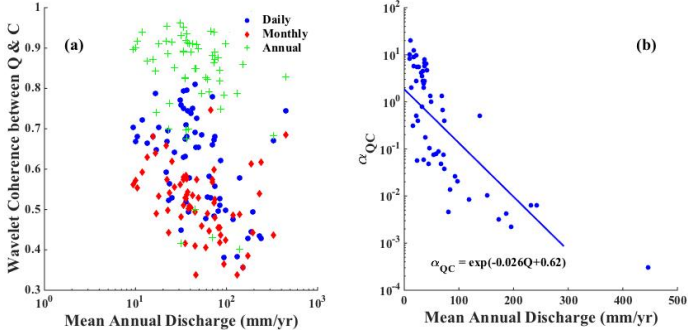
As we can see from Figure 1a and A3, the annual scale has largest wavelet coherence. The wavelet coherence is like the correlation coefficient, the larger it is, the more correlated the two variables are. Thus, we chose to use the annual for further analysis. We have made the following changes in the manuscript, we hope the reviewer finds our explanation sufficient (please see lines 133 – 135).

This analysis is applied only at annual scale since this is when the coupling from wavelet coherence analysis is the strongest (the one with the largest wavelet coherence).

(8) On line 141-142, “slope in the Q-C regression (aQC) declines exponentially with Q_m (p-value < 0.0001)”. From the Figure 1b, it looks like log-transformation used to aQC. If so, then the text expression and plot were inconsistent. And the authors should give the mathematical equation of exponential decline trend and its fitted curve.

Thank you for noticing the logarithmic scale in y axis. We chose to use logarithmic scale for the slope in Q-C regression to better present the differences among small values which is a large amount in the study catchment, otherwise the small values would just cluster together. Taking the log-transformation on both side of the exponential regression, we will have a linear relationship between $\log(\alpha_{QC})$ and Q . We have added the fitted curve and the equation in the updated Figure 1. We are sorry about the confusion and hope the reviewer will find our explanation satisfactory. Thank you!

Figure 1: Scatter plots between long-term mean annual discharge (Q_m) and (a) wavelet Q - C coherence at daily, monthly and annual scales, (b) slope of the discharge- sediment concentration regression (α_{QC}) at annual scale, $R^2 = 0.55$ and p -value < 0.0001 .



1 Emergent stationarity in Yellow River sediment transport and the
2 underlying shift of dominance: from streamflow to vegetation

3 Sheng Ye¹, Qihua Ran^{1*}, Xudong Fu², Chunhong Hu³, Guangqian Wang², Gary
4 Parker⁴, Xiuxiu Chen¹, Siwei Zhang¹

5

6 ¹ Institute of Hydrology and Water Resources, Department of Hydraulic Engineering,
7 Zhejiang University, Hangzhou 310058, China

8 ² State Key Laboratory of Hydro-science and Engineering, Tsinghua University,
9 Beijing 100084, China

10 ³ State Key Laboratory of Simulation and Regulation of Water Cycle in River Basin,
11 Institute of Water Resources and Hydropower Research, Beijing 100048, China

12 ⁴ Department of Civil & Environmental Engineering and Department of Geology,
13 University of Illinois at Urbana-Champaign, Urbana, Illinois 61801, USA

14 * Corresponding author: Qihua Ran (ranqihua@zju.edu.cn)

15

16 Submitted to: *Hydrology and Earth System Sciences*

17

18 ~~Nov 13th 2018~~

19

Deleted: May

Deleted: 5

22 **Abstract**

23 Soil erosion and sediment transport play important roles in terrestrial landscape
24 evolution and biogeochemical cycles of nutrients and contaminants. Although
25 discharge is considered to be a controlling factor in sediment transport, its correlation
26 with sediment concentration varies across the Yellow River Basin (YRB) and is not
27 fully understood. This paper provides analysis from gauges across the YRB covering
28 a range of climate, topographic characteristics and degree of human intervention. Our
29 results show that discharge control on sediment transport is dampened at gauges with
30 large mean annual discharge, where sediment concentration becomes more and more
31 stable. This emergent stationarity can be attributed to vegetation resistance. Our
32 analysis shows that sediment concentration follows a bell shape with vegetation index
33 (normalized difference vegetation index, NDVI) at annual scale despite heterogeneity
34 in climate and landscape. We obtain the counterintuitive result that as mean annual
35 discharge increases, the dominant control on sediment transport shifts from
36 streamflow erosion to vegetation retardation in the YRB.

37 **Keywords:** Yellow River Basin, sediment, stationarity, vegetation, bell-shape

38

39 **1. Introduction**

40 Watershed sediment transport, from hillslope to channel and subsequently the coast, is
41 crucial to erosion management, flood control, river delta development, and the
42 quantification of global biogeochemical cycles of materials such as organic
43 phosphorus, iron, and aluminum (Martin and Meybeck, 1979). During the 20th century,
44 human activities have significantly modified the landscape, leading to a reduction in
45 sediment yield and coastal retreat worldwide (Walling and Fang, 2003; Syvitski et al.,
46 2005). Known for its severe sediment problems, the Yellow River (YR) has been a
47 hotspot for studies on soil erosion and sediment transport for decades. Since the 1950s,
48 the annual sediment yield has reduced by 80% because of check dam construction and
49 ecosystem restoration such as the Grain-for-Green project, motivating discussion on
50 the necessity for further expansion of re-vegetation schemes (Chen et al., 2015).

51 Most studies on the physical mechanisms of soil erosion and sediment transport were
52 conducted in relatively small sub-catchments (Collins et al., 2004; Ran et al., 2012).
53 In order to interpret the patterns discovered at basin scale, then, it is essential to
54 understand the scaling effects of soil erosion and sediment transport. Specifically,
55 would the mechanisms identified at small scale also prevail at basin scale? If not,
56 what factors influence upscaling (Mutema et al., 2015; Song et al., 2016). However,
57 existing studies on the scaling effects of sediment transport are rather limited, and
58 show no significant spatial coherence in the scaling of sediment transport (Le
59 Bissonnais et al., 1998; Deasy et al., 2011; Song et al., 2016). Due to the great
60 heterogeneity in the YRB, scaling patterns could be different even within one tributary.

61 Taking the Wuding River as example, event mean concentration could decrease
62 downstream after the initial increase in one sub-catchment (Zheng et al., 2011) or
63 keep rising until reaching a plateau in another sub-catchment nearby (Fang et al.,
64 2008). Not only the sediment concentration, but also its correlation with discharge
65 varies across the YRB. Although discharge is considered as one of the controlling
66 factors in sediment transport, how its influence upscales remains to be fully
67 understood. Therefore it is necessary to expand our findings concerning sediment
68 transport from single tributaries to larger scales, especially incorporating diverse
69 climate, environmental and anthropogenic characteristics, so that we can derive an
70 understanding applicable to the whole YRB. In this paper, we collected observations
71 across the Yellow River Basin (YRB) to quantify changes in sediment concentration
72 in the recent decades (Rustomji et al., 2008; Miao et al., 2011; Wang et al., 2016). By
73 analyzing data from gauges across the YRB (Figure S1), we attempt to understand:
74 how the correlation between sediment concentration and discharge varies across
75 spatial and temporal scales; what are the dominant factors influencing sediment
76 transport in the YRB; and how their contributions vary from place to place.

77 2. Data and methodology

78 We collected daily discharge and sediment concentration data from 123 hydrology
79 gauges within our study area: the YRB above Sanmenxia station, the major
80 hydropower station on the YR. From these we selected 68 gauges spanning a range of
81 climate conditions and physiographic areas, from the gauge at the most upstream end

Deleted: A

83 of the main stem to the gauges above Tongguan, which just 100km upstream of
84 Sanmengxia Dam (Figure S1). These gauges were selected for at least 15-year (1971
85 – 1986) continuous daily discharge and sediment concentration records between 1951
86 and 1986. For comparison and further examination of our hypothesis, we also extract
87 the annual discharge and concentration data between 2000 and 2012 for seven gauges
88 located at the outlet of the major tributaries from the Yellow River Sediment Bulletin
89 (Figure S1 green stars).

Deleted: A

90 The vegetation data used in this study corresponds to the normalized difference
91 vegetation index (NDVI), which is an index calculated from remote sensing
92 measurements to indicate the density of plant growth (Running et al., 2004). The
93 NDVI data was downloaded from NASA's Land Long Term Data Record (LTDR)
94 project, which provides daily NDVI observations globally at a spatial resolution of
95 0.05°. Instead of the NDVI obtained from Global Inventory Modeling and Mapping
96 Studies (GIMMS), LTDR is chosen for its better estimation in the YRB (Sun et al.,
97 2015). The daily NDVI data from 44 gauges located on the eight major tributaries
98 were collected and extracted according to the drainage area of the study gauges from
99 1982 to 2012 (Figure S1 green stars). The gauges on the main stem of YR were not

Deleted: A

100 used as the water and sediment condition there is more likely controlled by the major
101 dams along the main stem rather than the hillslope characteristics. Annual maximum
102 NDVI values were used to represent the highest vegetation productivity. The
103 precipitation and leaf area index (LAI) data of the US catchments used for
104 comparison are assembled from the first author's previous work (Ye et al., 2015).

Deleted: A

108 To examine the coupling between discharge and sediment concentration at various
109 temporal scales, wavelet coherence analysis was applied to the daily discharge (m³/s)
110 and sediment concentration (kg/m³) data following Grinsted et al (2004). Wavelet
111 transforms decompose time series into time and frequency and can be used to analyze
112 different parts of the time series by varying the window size. They have been applied
113 to geophysical records for the understanding of variability at temporal scales. To
114 examine the co-variation between discharge and concentration in the time frequency
115 domain, we used a wavelet coherence defined as (Grinsted et al 2004)

$$116 \quad R^2(s) = \frac{|S(s^{-1}W^{XY}(s))|^2}{S(s^{-1}|W^X(s)|^2) * S(s^{-1}|W^Y(s)|^2)} \quad (1)$$

117 where S is a smoothing operator, W^{XY} is cross wavelet transform of time series X and
118 Y representing the common power between the two series, s refers to scale and W^X
119 and W^Y are the continuous wavelet transforms of time series X and Y respectively.
120 The wavelet coherence can be considered as a correlation coefficient of the two time
121 series in the time frequency domain. The region of cone of influence (COI) was
122 delineated in the wavelet coherence images to avoid reduction in confidence caused
123 by edge effects. Localized wavelets were also averaged through temporal scales to
124 obtain global wavelet coherence (Guan et al., 2011). More detailed explanation about
125 wavelet coherence analysis can be found in Grinsted et al (2004).

126 The annual discharge (Q_a) and the sediment yield (L_a) were aggregated from daily to
127 further examine their correlation:

Deleted: discharge x concentration

Deleted: annually to

130 $Q_a = (\sum_{i=1}^n(Q_i * 3600 * 24))/Ad * 1000$ (2)

131 $L_a = (\sum_{i=1}^n(Q_i * C_i * 3600 * 24))$ (3)

132 where Q_i (m³/s) and C_i (kg/m³) are the daily discharge and sediment concentration, Ad
133 is the drainage area (km²) of each gauge, n is the number of days in each year. This
134 analysis is applied only at annual scale since this is when the coupling from wavelet
135 coherence analysis is the strongest (the one with the largest wavelet coherence). The
136 annual mean concentration (C_a) was calculated as:

137 $C_a = L_a/(Q_a * Ad/1000)$ (4)

138 The long-term mean annual discharge (Q_m) and the long-term mean annual
139 concentration (C_m) was also calculated by averaging for the period of 1951 to 1986.

140 Note that both the parameters Q_a and Q_m used here are area-specific discharges
141 (mm/yr). For each gauge, a linear regression was fit to describe the correlation
142 between annual discharge (Q_a) and annual mean concentration (C_a). The slope of this
143 linear regression (α_{QC}) is used to describe the rate of change in sediment
144 concentration with changing discharge at annual scale.

145 **3. The emergent stationarity in sediment concentration**

146 We applied wavelet coherence analysis to daily discharge and sediment concentration
147 data at 68 study gauges across the YRB (Figure S2, S3). The results show that the
148 coupling between discharge and concentration (Q-C) declines with mean annual
149 discharge (Q_m) at all three temporal scales (Figure 1a). That is, as Q_m increases, the
150 influence of streamflow on sediment transport becomes weaker and weaker, both at

Deleted: by dividing the annual sediment yield by annual discharge.

Deleted: annual discharge (Q_a) and annual mean concentration (C_a) was also averaged within the period 1951 to 1986 to obtain the

Deleted: A

Deleted: A

158 intra-annual and within-year scales.

159 This fading impact of streamflow as it increases can be further quantified in terms of a
160 linear regression between discharge (Q_d) and mean sediment concentration (C_a) at
161 annual scale, when the coupling between discharge and concentration (Q-C) is the

162 strongest (Figure S4). As can be seen from Figure 1b, though annual mean

Deleted: A

163 concentration is positively correlated with annual discharge at most gauges, the slope

164 in the Q-C regression (α_{QC}) declines exponentially with Q_m (p -value < 0.0001). The

165 larger Q_m is, the less sensitive sediment concentration responds to variation in annual

166 discharge. For example, gauges with α_{QC} less than 0.1 are the ones with Q_m larger

Deleted: most gauges

167 than 60mm/yr. When Q_m is larger than 100mm/yr, the variation in sediment

Deleted: , α_{QC} is less than 0.1

168 concentration is less than 1% of that in streamflow ($\alpha_{QC} < 0.01$), and thus sediment

169 concentration can be approximated as invariant to changing discharge. Most of these

170 gauges locate on the main stem or near the outlets of tributaries. This increased

171 independence between sediment concentration and discharge may be attributed to the

172 heterogeneity in these relatively large catchments.

173 This emergent stationarity explains the linear correlation between area-specific

174 sediment yield and runoff depth reported in a small sub-watershed in a hilly area of

175 the Loess Plateau (Zheng et al., 2013). Considering the sediment concentration to be

176 constant, the variation in yield is solely dominated by streamflow, resulting in the

177 observed linear discharge-yield relationship. Similar stationarity in sediment

178 concentration has also been found in arid watersheds in Arizona (Gao et al., 2013), US

182 where the sediment concentration becomes homogeneous among watersheds when
183 their drainage area is larger than 0.01 km². The difference in threshold for the
184 emergence of approximately discharge-invariant concentration between the YRB and
185 watersheds in Arizona, US is probably due to the differences in catchment
186 characteristics, i.e. vegetation type and coverage, terrestrial structure, soil properties,
187 etc.

188 Our analysis shows that mean annual discharge (Q_m) is a better indicator of the
189 correlation between water and sediment transport than drainage area, although the last
190 parameter has been used traditionally. Despite the heterogeneity, both the coupling
191 between Q-C and the concentration sensitivity to variation in streamflow decreases
192 with Q_m . A closer inspection reveals useful insights. At gauges with smaller values of
193 Q_m , discharge is the dominant factor in sediment transport: an increment in annual
194 discharge is amplified in the increment of sediment concentration ($\alpha_{QC} > 1$) (i.e.
195 Gauge 808, 812 in Figure S4). However, as Q_m increases, variation in streamflow is
196 more weakly reflected in variation in sediment concentration, even though annual
197 mean concentration still correlates with annual discharge, (i.e. Gauge 806 in Figure
198 S4). As Q_m continues to increase, sediment concentration becomes almost invariant to
199 discharge, suggesting that the dominant factor of sediment transport has shifted from
200 the discharge to something else.

201 4. The vegetation impact: a bell shape

202 To further explore the potential cause of this emergent stationarity, we analyzed the

Deleted: A

Deleted: A

205 vegetation data (NDVI) from 44 of the gauges locating on eight major tributaries of
206 the YR (Figure S1). Our analysis shows that this declining sensitivity in concentration
207 at annual scale (α_{QC}) is negatively related to vegetation impact (Figure 2).

Deleted: A

208 For gauges with limited vegetation establishment in their drainage area, the variation
209 in discharge is amplified in sediment transport ($\alpha_{QC}>1$). The larger the discharge is at
210 specific year, the more sediment is eroded and mobilized per cubic meter. This
211 dominance of discharge is weakened when vegetation density and coverage increase.
212 Despite the larger sediment carrying capacity of larger discharge, sediment
213 concentration is reduced, probably due to the protection vegetation offers against
214 erosion. As maximum NDVI increase, sediment concentration becomes less and less
215 coupled with discharge at annual scale. When the vegetation density is sufficiently
216 high, sediment concentration is nearly stable in spite of the variation in discharge,
217 since the dense vegetation coverage protects soil from erosion and traps sediment.
218 That is, the emergent stationarity in sediment concentration corresponding to the
219 variation in discharge at gauges with large Q_m can be attributed to the dampened
220 dominance of discharge due to the increasing impact of vegetation retardation.

221 To further confirm the vegetation impact on sediment transport, we derived the plot
222 between maximum NDVI and mean concentration at annual scale in Figure 3a. As we
223 can see, the annual mean sediment concentration follows a bell-shaped correlation
224 with vegetation establishment, with a peak concentration at a value of maximum
225 NDVI of around 0.36. On the falling limb of this bell curve, as NDVI increases, both

227 sediment concentration and α_{QC} decrease consistently. That is, both the value of
228 concentration and its sensitivity to streamflow variation declines with increasing
229 vegetation index on the falling limb. To confirm this impact of vegetation resistance,
230 we also examined the relationship between sediment concentration and other
231 catchment characteristic like dominant soil type. No significant correlation was
232 observed as vegetation did. Although there could still be other factors not considered
233 here contributed to the decline in sediment concentration, it is undoubted that
234 vegetation is one of the most influential factors of sediment reduction and can be used
235 as a good indicator of the soil erosion and sediment transport in the YRB.

236 On the rising limb, however, both the value of concentration and its sensitivity to
237 streamflow variation increases with increasing vegetation index. Most gauges have
238 values α_{QC} larger than one, except one gauge with an extremely small maximum
239 value of NDVI. For these gauges, on the rising limb, vegetal cover is still low in an
240 absolute sense despite increasing NDVI. Sediment concentration is mainly dominated
241 by discharge: fluctuations in streamflow are amplified in concentration ($\alpha_{QC}>1$). The
242 only gauge with a value of α_{QC} smaller than one is gauge HanJiaMao (HJM) at the
243 Wuding River. Although the annual precipitation and discharge at HJM is similar to
244 other gauges along the Wuding River, the annual mean sediment concentration is
245 much smaller. This is because of the extremely high baseflow contribution in
246 discharge at HJM, which is around 90%, thanks to very intensive check-dam
247 construction there (Dong and Chang, 2014). Since sediment in the YRB is mostly
248 transported during large flow events during the summer, smaller flow events are not

249 capable of transporting significant sediment loads at HJM.

250 In general, we can conclude that sediment transport is mainly dominated by discharge
251 when the vegetation index is low. With increasing NDVI, the impact of vegetation
252 grows slowly at first, and accelerates after the maximum NDVI exceeds 0.36.
253 Eventually, the effect of NDVI takes over the dominance of streamflow, and
254 attenuates the variation in sediment concentration (Figure 4). The nonlinear impact of
255 vegetation in regard to resistance of sediment to erosion is consistent with previous
256 findings (Rogers and Schumm, 1991; Collins et al., 2004; Temmerman et al., 2005;
257 Corenblit et al., 2009). When the vegetation index level is low, its resistance to soil
258 erosion develops slowly as vegetation grows and expands (Rogers and Schumm,
259 1991), and capability of vegetation to trap sediment is reduced when submerged by
260 flood (Temmerman et al., 2005) or overland flow. Therefore, for catchments with
261 limited vegetation establishment, the coverage of vegetation is insufficient to trap
262 sediment, nor is the vegetation able to protrude from the water level during the
263 extreme flow events that transport most of the sediment. Sediment transport in these
264 catchments is usually dominated by discharge. As NDVI increases, vegetation
265 becomes much more capable as an agent of erosion protection and sediment settling
266 (Jordanova and James 2003; Corenblit et al., 2009). With the compensation from
267 vegetation retardation, sediment and discharge become more and more decoupled as
268 discharge increases, so that concentration is nearly invariant to increasing discharge.
269 The transition point in maximum NDVI (around 0.36) is where the increment in
270 vegetation reduction balances with the incremental increase in water erosion. When

271 the capability of vegetation retardation catches up with streamflow erosion, the net
272 soil loss becomes negligible, a condition commonly observed in well-vegetated
273 regions.

274 **5. Validation of the bell shape across time and space**

275 Since 1999, a large-scale ecosystem restoration project, the ‘Grain-for-Green’ project
276 was launched in the YRB for soil conservation (Lv et al., 2012). It has substantially
277 improved vegetation coverage after a decade of implementation (Sun et al., 2015). To
278 validate our hypothesis gain from the early 1980s, we applied similar analysis to the
279 annual flow and sediment data as well as daily NDVI data at seven gauges located at
280 the outlets of major tributaries from 2008 to 2012 (Figure S1 green stars). This is the
281 period subsequent to the initiation of the ‘Grain-for-Green’ project. We have excluded
282 the years right after the implementation of the ‘Grain-for-Green’ project, when there
283 was an initial drastic change in vegetation coverage and sediment erosion and
284 transport processes.

285 As we can see from Figure 3b, there is significant increase in maximum NDVI for all
286 seven catchments, and considerable reduction in mean sediment concentration. This
287 improvement is consistent with the previous report that the ‘Grain-for-Green’ project
288 has made a remarkable achievement in regard to soil conservation in the YRB (Chen
289 et al., 2015). Comparison of the relationship between sediment concentration and
290 maximum NDVI in the early 1980s and around 2010 shows that the bell shape
291 relationship sustains even after drastic and significant anthropogenic alteration of the

Deleted: A

293 land use and land cover across the whole YRB. Although the vegetation coverage has
294 improved significantly at all seven comparison gauges due to the ecosystem
295 restoration policy, and thereby effectively moderated sediment erosion; the bell shape
296 relationship between maximum NDVI and mean concentration sustains.

297 Similar bell shape relationship was also found for the multi-year mean annual
298 precipitation and sediment yield observed in the United States (Langbein and Schumm,
299 1958). The data used in the analysis of Langbein and Schumm (1958) was collected in
300 the 1950s from more humid and vegetated catchments with limited human
301 intervention, on the opposite of the YRB. Yet similar bell shape was still observed
302 between sediment yield and precipitation. Given the limited anthropogenic activities
303 in these catchments, vegetation growth is probably to correlate with annual
304 precipitation due to its adaption to climate, as in other US catchments (Figure S6).

305 Thus it is likely that a bell shape correlation between vegetation and sediment yield
306 would be found at these US catchments as well. This suggests that the bell shape
307 correlation between vegetation and sediment concentration is not only observed in the
308 YRB with intensive human intervention, but could also be valid outside it. More
309 analyses are needed to test this relationship in other catchments outside the YRB for
310 its universality.

311 6. Implications and conclusion

312 Our analysis shows that across the YRB, both the correlation between Q and C and
313 the magnitude of sediment response to the variation in streamflow decreases with Q_m .

Deleted: A

Deleted: 6

316 When Q_m is sufficiently large (i.e. > 60 mm/yr), sediment concentration reaches a
317 stationary (constant) state at annual scale. The emergent stationarity at gauges with
318 large Q_m is related to the shift of dominance from discharge to vegetation. Because of
319 the slow development of vegetation resistance with increasing discharge for small
320 discharges, discharge dominates the soil erosion and sediment transport process until
321 the maximum NDVI exceeds a threshold (0.36 for this study), at which the parameter
322 governing concentration transits from streamflow erosion to vegetation retardation.

323 Our findings of the emergent stationarity in sediment concentration and the shift of
324 the dominant mechanism governing the Q-C relation have important implications for
325 water and sediment management at watershed scale. Our study indicates that for the
326 gauges with relatively large discharge, the annual mean concentration can be
327 approximated as a constant over a large range of discharges. Thus the estimation of
328 sediment yield can be simply inferred from a simulation of streamflow. First order
329 estimates of sediment yield for scientific or engineering purposes can be obtained by
330 multiplying the estimated discharge by a constant sediment concentration estimated
331 based upon the vegetation index. The correlation between vegetation and sediment
332 concentration will also be useful for the design of the ongoing ecosystem restoration
333 program known as the 'Grain-for-Green' project. The bell-shaped correlation between
334 maximum NDVI and sediment concentration provides a quantitative way to estimate
335 the potential change in sediment concentration associated with proposed ecosystem
336 restoration planning schemes at and near each tributary. This can help guide land use
337 management so as to allocate the sediment contribution from each of the upstream

338 tributaries in a way that maintains the balance between erosion and deposition in the
339 lower YR.

340 It is important to collect more data from the current decade (i.e. after the substantial
341 ecosystem restoration) to further validate our findings in regard to emergent
342 stationarity and vegetation impact at more gauges in the YRB. It will be helpful if we
343 could examine our findings in other watersheds worldwide with different climate and
344 vegetation types. Although humid regions are usually considered as well-vegetated,
345 study shows that there could still be erosion issues in these areas due to topographic
346 gradient, precipitation intensity, and soil properties, etc. (Holz et al., 2015). Analysis
347 with more field measurements could also help explain the threshold discharge of the
348 emergent stationarity. Numerical simulations as well as long-term measurements on
349 the soil properties are also needed to further explain the physical mechanism of
350 vegetation retardation; how it develops its impact on soil erosion and sediment
351 transport by changing soil properties and other topographic characteristics during its
352 growth and spread.

Deleted: as well as

Deleted:

Deleted: detailed

Deleted: ,

Deleted: including

Deleted: develops and how it upscales

353 Acknowledgements

354 This research was financially supported by the National Key Research and
355 Development Program of China (2016YFC0402404, 2016YFC0402406) and the
356 National Natural Science Foundation of China (51509218, 51379184, 51679209). All
357 the data used in this study were downloaded from websites indicated in Materials and
358 Methods section in Supplementary. The authors thank Dr. Jinren Ni for insightful
359 discussion.

360 References

367 Chen, Y. P., K. B. Wang, Y. S. Lin, W. Y. Shi, Y. Song, and X. H. He (2015),
368 Balancing green and grain trade, *Nat Geosci* 8: 739-741.

369 Collins, D. B. G., R. L. Bras, and G. E. Tucker (2004), Modeling the effects of
370 vegetation-erosion coupling on landscape evolution, *J Geophys Res* 109: 121 –
371 141.

372 Corenblit, D., J. Steiger, A. M. Gurnell, E. Tabacchi, and L. Roques (2009), Control of
373 sediment dynamics by vegetation as a key function driving biogeomorphic
374 succession within fluvial corridors. *Earth Surf Process Landforms* 34: 1790–1810.

375 Deasy, C., S. A. Baxendale, A. L. Heathwaite, G. Ridall, R. Hodgkinson, and R. E.
376 Brazier (2011), Advancing understanding of runoff and sediment transfers in
377 agricultural catchments through simultaneous observations across scales, *Earth*
378 *Surf Process Landforms* 36: 1749–1760.

379 Dong, J and L. Chang (2014), Analysis of runoff characteristic change and influence
380 for Hailiutu River, *J Water Resour. & Water Eng* 25: 143 – 147.

381 Fang, H. Y., Q. G. Cai, H. Chen, and Q. Y. Li (2008), Temporal changes in suspended
382 sediment transport in a gullied loess basin: The lower Chabagou Creek on the
383 Loess Plateau in China. *Earth Surf Process Landforms* 33: 1977–1992.

384 Gao, P., M. A. Nearing, and M. Commons (2013), Suspended sediment transport at
385 the instantaneous and event time scales in semiarid watersheds of southeastern
386 Arizona, USA. *Water Resour Res* 49: 6857–6870.

387 Grinsted, A., S. Jevrejeva, and J. Moore (2004), Application of the cross wavelet
388 transform and wavelet coherence to geophysical time series. *Nonlinear Proc*

389 *Geoph* 11: 561–566.

390 Guan, K., S. E. Thompson, C. J. Harman, N. B. Basu, P. S. C. Rao, M. Sivapalan, A. I.

391 Packman, and P. K. Kalita (2011), Spatiotemporal scaling of hydrological and

392 agrochemical export dynamics in a tile-drained Midwestern watershed. *Water*

393 *Resour Res* 47: 1290 – 1300.

394 Holz, D. J., K. W. J. Williard, P. J. Edwards, J. E. Schoonover (2015), Soil erosion in

395 humid regions: a review. *J Contemp Water Res Educ* 154: 48-59.

396 Jordanova, A. A., and C. S. James (2003), Experimental Study of Bed Load Transport

397 through Emergent Vegetation. *J Hydraul Eng* 129: 474-478.

398 Langbein, W. B., and S. A. Schumm (1958), Yield of sediment in relation to mean

399 annual precipitation, *Eos Trans. AGU*, 39(6), 1076-1084.

400 Le Bissonnais, Y., H. Benkhadra, V. Chaplot, D. Fox, D. King, and J. Daroussin

401 (1998), Crusting, runoff and sheet erosion on silty loamy soils at various scales

402 and upscaling from m² to small catchments. *Soil Tillage Res* 46: 69–80.

403 Lv, Y., B. Fu, X. Feng, Y. Zeng, Y. Liu, R. Chang, G. Sun, and B. Wu (2012), A

404 policy-driven large scale ecological restoration: quantifying ecosystem services

405 changes in the Loess Plateau of China. *PloS One*, 7 (2), e31782.

406 Martin, J. M. and M. Meybeck (1979), Elemental mass-balance of material carried by

407 major world rivers. *Mar Chem* 7: 173 – 206.

408 Miao, C. Y., J. R. Ni, A. G. L. Borthwick, and L. Yang (2011), A preliminary estimate

409 of human and natural contributions to the changes in water discharge and

410 sediment load in the Yellow River. *Global Planet Change* 76: 196–205.

Formatted: Justified, Line spacing: Double

Formatted: Font: Italic

Formatted: Font: (Default) Times, (Asian) +Body Asian (SimSun), Font color: Black

Deleted: ¶

412 Mutema, M., V. Chaplot, G. Jewitt, P. Chivenge, and G. Bloschl (2015), Annual
413 water, sediment, nutrient, and organic carbon fluxes in river basins: A global
414 meta-analysis as a function of scale. *Water Resour Res* 51: 8949– 8972.

415 Ran, Q., D. Su, P. Li, and Z. He (2012), Experimental study of the impact of rainfall
416 characteristics on runoff generation and soil erosion. *J Hydrol* 424 – 425: 99 –
417 111.

418 Rogers, R. D., and S. A. Schumm (1991), The effect of sparse vegetative cover on
419 erosion and sediment yield. *J Hydrol* 123: 19–24.

420 [Running, S. W., F. A. Heinsch, M. Zhao, M. Reeves, H. Hashimoto, and R. R. Nemani](#)
421 [\(2004\), A continuous satellite-derived measure of global ter- restrial primary](#)
422 [production, *Bioscience*, 54\(6\), 547–560, doi:10.1641/](#)
423 [0006-3568\(2004\)054\[0547:ACSMOG\]2.0.CO;2.](#)

424 Rustomji, P., X. P. Zhang, P. B. Hairsine, L. Zhang, and J. Zhao (2008), River
425 sediment load and concentration responses to changes in hydrology and catchment
426 management in the Loess Plateau of China. *Water Resour Res* 44: 148 - 152.

427 Song, C., G. Wang, X. Sun, R. Chang, and T. Mao (2016), Control factors and scale
428 analysis of annual river water, sediments and carbon transport in China. *Sci Rep* 6:
429 25963.

430 Sun, W., X. Song, X. Mu, P. Gao, F. Wang, and G. Zhao (2015), Spatiotemporal
431 vegetation cover variations associated with climate change and ecological
432 restoration in the Loess Plateau. *Agr Forest Meteorol* 209-210: 87–99.

433 Syvitski, J. P. M., C. J. Vorosmarty, A. J. Kettner, and P. Green (2005), Impact of

Formatted: Space After: 0 pt, Line spacing: Double

434 humans on the flux of terrestrial sediment to the global coastal ocean. *Science* 308:
435 376–380.

436 Temmerman, S., T. J. Bouma, G. Govers, Z. B. Wang, M. B. De Vries, and P. M. J.
437 Herman (2005), Impact of vegetation on flow routing and sedimentation patterns:
438 Three-dimensional modeling for a tidal marsh. *J Geophys Res* 110: 308 – 324.

439 Walling, D. E. and D. Fang (2003), Recent trends in the suspended sediment loads of
440 the world’s rivers. *Global Planet Change* 39: 111 – 126.

441 Wang, S., B. Fu, S. Piao, Y. Lv, C. Philippe, X. Feng, and Y. Wang (2016), Reduced
442 sediment transport in the Yellow River due to anthropogenic changes. *Nat Geosci*
443 9: 38-41.

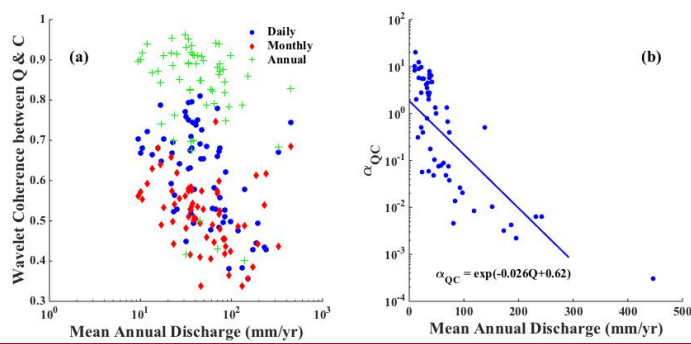
444 Ye, S., H.-Y. Li, S. Li, L. R. Leung, Y. Demissie, Q. Ran, and G. Blöschl (2015),
445 Vegetation regulation on streamflow intra-annual variability through adaption to
446 climate variations, *Geophys. Res. Lett.*, 42, 10,307–10,315, doi:10.1002/
447 2015GL066396.

448 Zheng, M. G., F. Qin, L. Y. Sun, D. L. Qi, and Q. G. Cai (2011), Spatial scale effects
449 on sediment concentration in runoff during flood events for hilly areas of the
450 Loess Plateau, China. *Earth Surf Process Landforms* 36: 1499–1509.

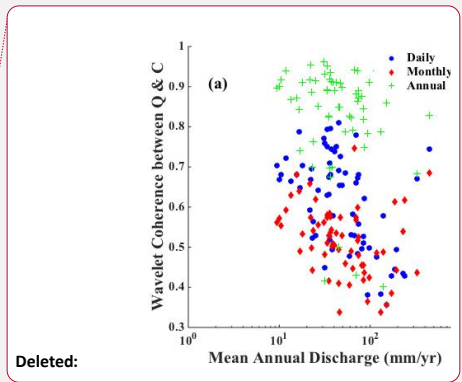
451 Zheng, M. G., F. Qin, J. S. Yang, and Q. G. Cai (2013), The spatio-temporal
452 invariability of sediment concentration and the flow–sediment relationship for
453 hilly areas of the Chinese Loess Plateau. *Catena* 109: 164–176.

454

455 **Figure 1:** Scatter plots between long-term mean annual discharge (Q_m) and (a)
 456 wavelet Q - C coherence at daily, monthly and annual scales, (b) slope of the discharge-
 457 sediment concentration regression (α_{QC}) at annual scale, $R^2 = 0.55$ and p -value <
 458 0.0001.



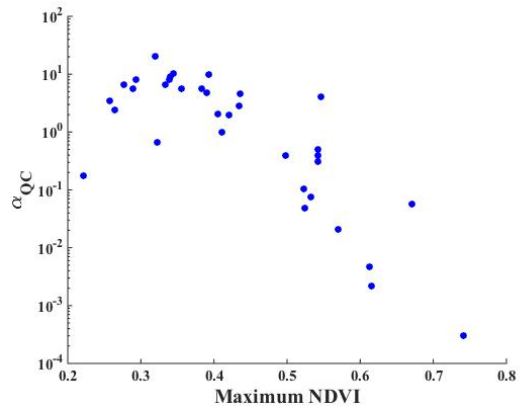
Formatted: Superscript
 Formatted: Font: Italic



460
 461

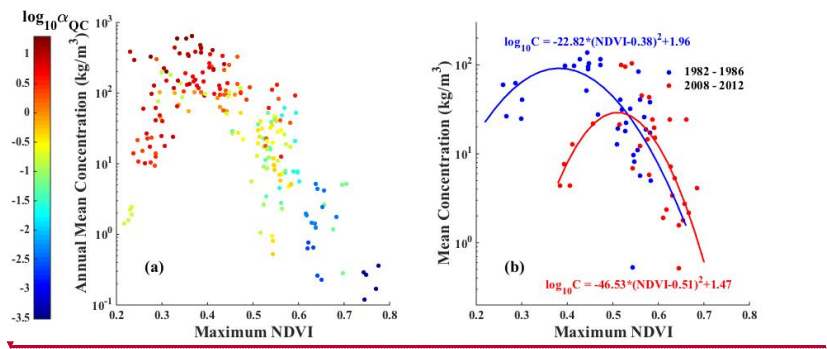
463 **Figure 2:** Scatter plots between the maximum NDVI and slope in the Q-C regression

464 (α_{QC}).

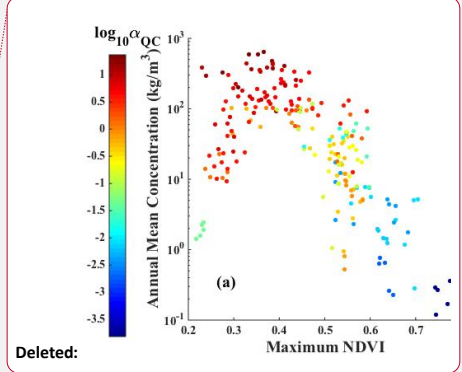


465

466 **Figure 3.** Scatter plot of annual mean concentration and maximum NDVI: (a) at 44
 467 study gauges between 1982 and 1986, where the dots are color-coded by the slope in
 468 the Q-C regression (α_{QC}) at each gauge; and (b) at 7 gauges with both data from the
 469 years 1982 – 1986 (blue dots) and the years 2008 – 2012 (red dots). *The R^2 for the*
 470 *two fit is 0.6 and 0.44 respectively with p -value < 0.001 for both of them.*

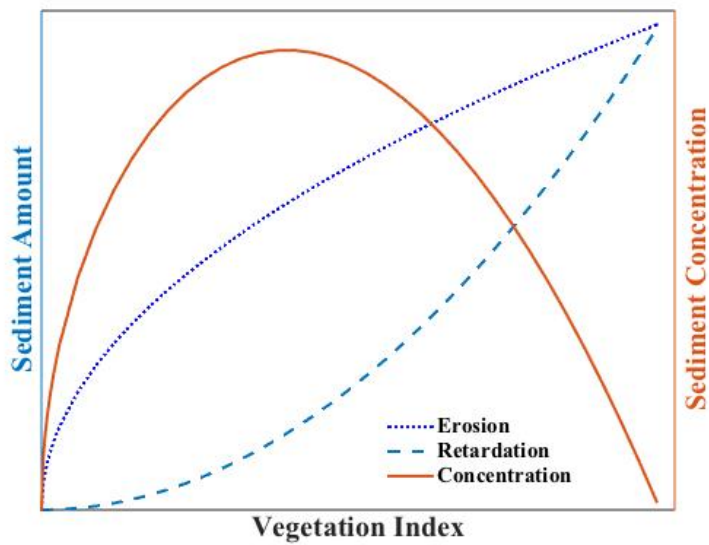


Formatted: Superscript
 Formatted: Font: Italic



471

473 **Figure 4.** Illustration of the correlation between vegetation and sediment erosion,
474 retardation and the resulting sediment concentration in the YRB. Since vegetation
475 usually increases with discharge, with the rise in discharge, sediment eroded and
476 delivered by streamflow increases rapidly, while the retardation from vegetation is
477 limited at the beginning and increases fast afterwards. This non-synchronous impact
478 on sediment transport leads to the bell shape correlation between sediment
479 concentration and vegetation.



480

481

482

483

Supplementary

484

Figure S1: Spatial distribution of hydrology gauges used in this study. The green

485

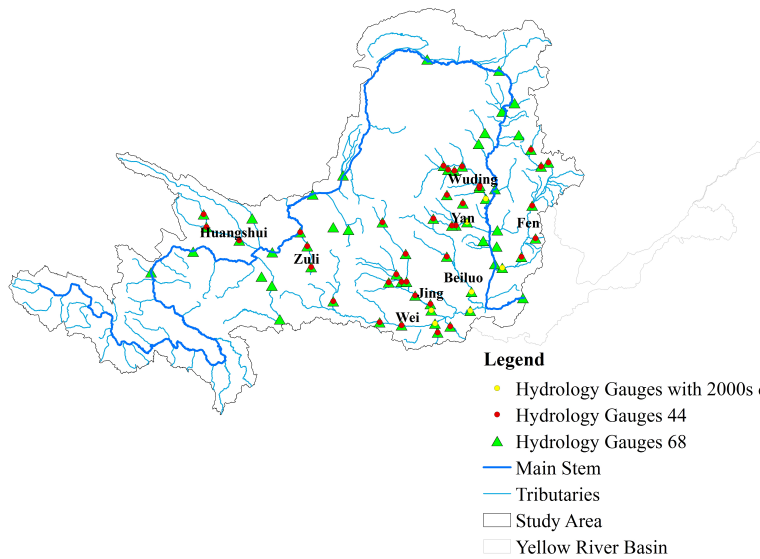
triangles correspond to 68 gauges with discharge and sediment concentration data, the

486

red circles correspond to 44 selected gauges with NDVI data, and the yellow circles

487

are the ones with annual discharge and sediment data for the years 2000 – 2012.



488

Deleted: Appendix

Deleted: ¶

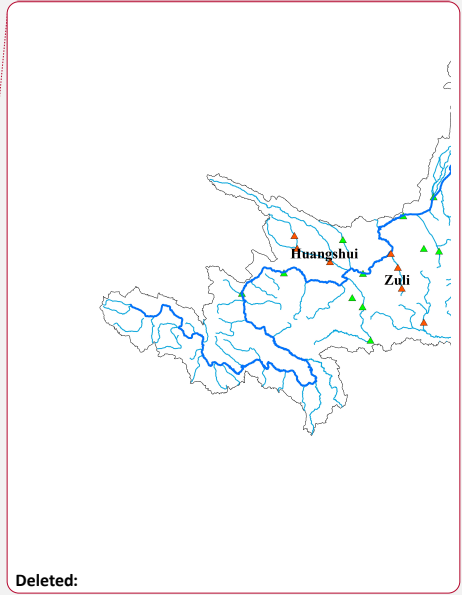
Deleted: A

Formatted: Font: Not Bold

Deleted: triangles

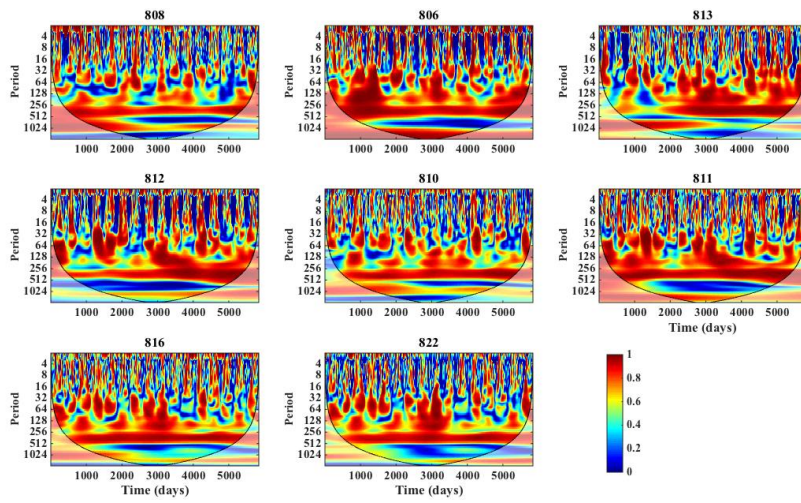
Deleted: green

Deleted: stars



496 **Figure S2:** Wavelet coherence plots of the coupling between standardized discharge
497 and concentration, using the Jing River as an example. The labels correspond to the
498 gauge IDs. The shaded area is the cone of influence (COI) of edge effects.

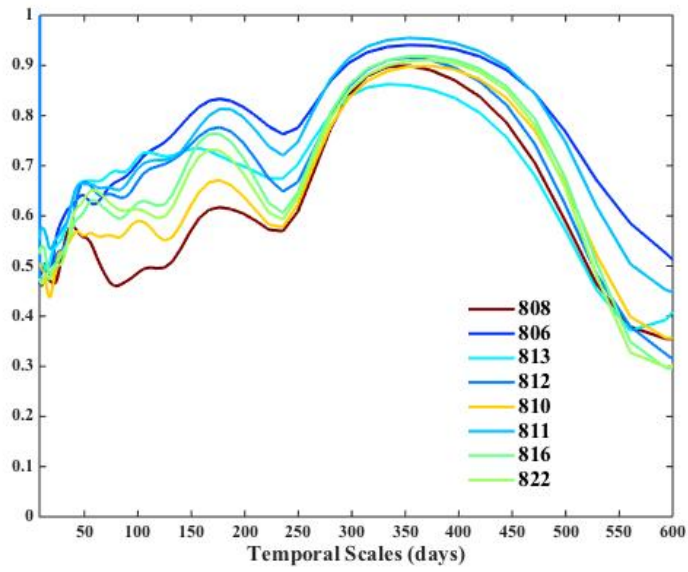
Deleted: A



499

501 **Figure S3:** Averaged wavelet coherence plot, using the Jing River as an example. The
502 lines are colored according to long-term mean annual discharge (mm/yr), from blue to
503 brown as discharge increases.

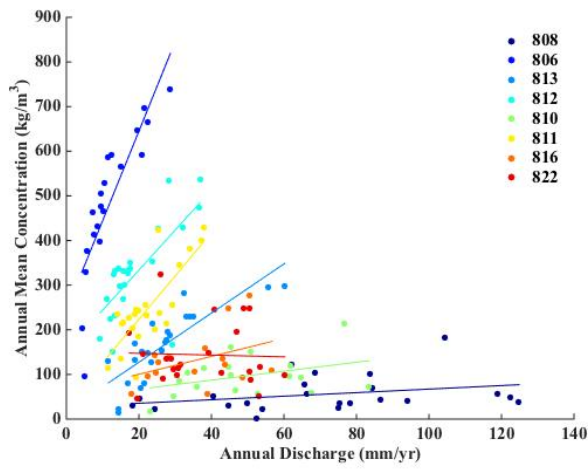
Deleted: A



504
505

507 **Figure S4:** Scatter plot of the annual discharge and annual mean concentration from
508 1951 to 1986, as well as the result of linear regression between discharge and
509 concentration, using the gauges along the Jing River as an example.

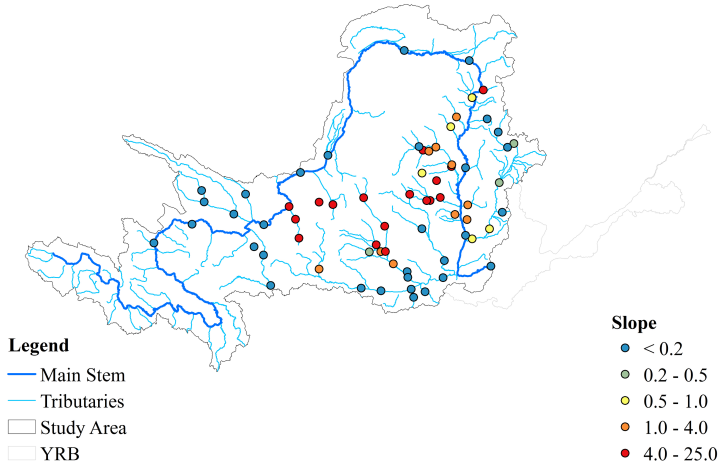
Deleted: A



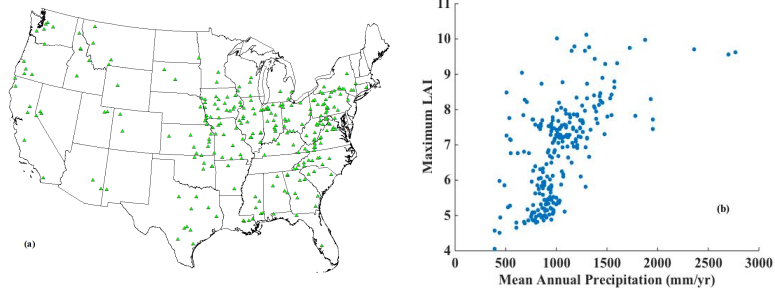
510

Figure S5: Spatial distribution of the slope of the Q-C regressions (α_{QC}).

Deleted: A



515 **Figure S6.** a) Spatial distribution of the MOPEX catchments; b) scatter plot of mean
516 annual precipitation and annual maximum LAI for the MOPEX catchments.



517

Deleted: ¶
Column Break
Deleted: A
Deleted: 6